# Coherent activation of a steerability-breaking channel

Huan-Yu Ku,[1,2,*,†] Kuan-Yi Lee,[3,4,*] Po-Rong Lai,[3,4] Jhen-Dong Lin,[3,4] and Yueh-Nan Chen[3,4,‡]

[1]*Faculty of Physics, University of Vienna, Boltzmanngasse 5, 1090 Vienna, Austria*

[2]*Institute for Quantum Optics and Quantum Information (IQOQI), Austrian Academy of Sciences, Boltzmanngasse 3, 1090 Vienna, Austria*

[3]*Center for Quantum Frontiers of Research and Technology (QFort), National Cheng Kung University, Tainan 701, Taiwan*

[4]*Department of Physics, National Cheng Kung University, Tainan 701, Taiwan*

(Received 10 October 2022; revised 12 February 2023; accepted 31 March 2023; published 12 April 2023)

The inevitable noise within one-sided device-independent quantum information tasks may completely break any steering resources. These noisy effects are characterized by the steerability breaking (SB) channels. In this work, we demonstrate the use of a control system that can superpose $N$ copies of the given SB channel to activate SB channels such that the channel becomes a non-SB one. In particular, we analytically and numerically show that the SB depolarizing and amplitude-damping channel can be coherently activated when $N \geqslant 2$. In addition, for both cases, the channels can preserve more steerability when increasing $N$. Finally, we propose circuit models to implement our proposed approaches and present the simulation results.

DOI: 10.1103/PhysRevA.107.042415

## I. INTRODUCTION

Quantum steering refers to a phenomenon in which one party (say, Alice) can affect another distant party (say, Bob) by her black-box measurements [1–5]. It has been shown that quantum steering is strongly related to many important features in quantum physics. For instance, (1) there is a one-to-one mapping between steering and measurement incompatibility [6–10], and (2) quantum steering is an intermediate correlation between entanglement [11–13] and Bell nonlocality [14–17]. A large variety of applications based on quantum steerability (also called one-sided device-independent quantum information tasks) has been reported experimentally [18–24], including quantum key distribution [25], quantum random number generation [26,27], subchannel-discrimination problems [28,29], and quantum metrology [30]. To take advantage of these tasks, many protocols on the quantification [31–35] and manipulation of quantum steerability have been proposed, e.g., the superactivation of quantum steering [36–38] and distillation of quantum steering [39–41].

Recently, many generalizations of quantum steering have been proposed to characterize the properties of a quantum channel [42–45]. An example is an undesired quantum channel, denoted as a steerability-breaking (SB) channel [46–49], for steering-based applications. An SB channel is conceptually defined in a similar way as the entanglement-breaking channel [50–52] but the focus is on steerability (see also the cases on high-dimensional steering [53,54]). For instance, if a quantum channel completely depolarizes the system, any steering resource [32] will be broken after the channel. Intuitively, SB channels are not useful for one-sided device-independent quantum information tasks. Similar to the hierarchy relation among entanglement, quantum steering, and Bell nonlocality [55,56], an SB channel must be entanglement breaking [57–59] but not necessarily nonlocality breaking [60–62].

In this work, we investigate a method to "coherently" activate SB channels by utilizing a coherently controlled system [63–68]. In other words, an SB channel is coherently activated if a quantum ancillary system can improve an undesired property of the channel such that it becomes non-SB. The framework involves a set of quantum channels and a quantum system that serves as control to determine which channel to apply. As shown in Fig. 1, the quantum system can be transmitted through $N$ copies of channels in a superposition manner. The ancillary system is a scheme that can therefore be regarded as a quantum extension of channel multiplexing; such schemes been applied to a wide range of disciplines, including quantum communication [69–74], relativistic quantum theory [75–77], and open quantum systems [78–81].

Here, we analytically and numerically show that the SB depolarizing and the SB amplitude-damping channels can be coherently activated when $N \geqslant 2$. In addition, when the copies of these channels increase, the steering preservability of both cases can be enhanced. Here, the channel preservability denotes the ability to maintain the quantum resource [82]. Therefore, using a quantum ancillary system, the undesired channel for steering-based tasks can now be used to transmit the steering resource within the task. Finally, to extend our approach to a practical level, we propose circuit models for the coherent activation of SB channels and present the simulation results.

This paper is organized as follows. In Sec. II, we summarize the basic notions, including quantum steering, SB channels, and coherently controlled system. In Sec. III, we present our main results by providing two examples for the

*These authors contributed equally.

†huan-yu.ku@oeaw.ac.at

‡yuehnan@mail.ncku.edu.tw

 

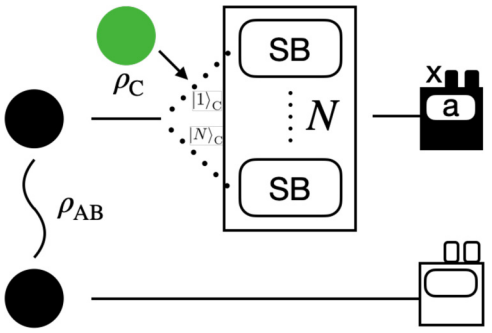


FIG. 1. A steerability-breaking (SB) channel breaks the quantum steerability of any bipartite quantum state $\rho_{AB}$ (black balls) with Alice's measurement assemblage (black box with input $x$ and outcome $a$). Bob's measurement is fully characterized. Now, we consider $N$ copies of the SB channel in which each channel is assigned by an associated-ancilla system (green ball) from a computational basis, i.e., $|1\rangle_C$. We test whether the SB channel can be coherently activated when one prepares the ancilla system in $\sum_i |i\rangle /\sqrt{N}$.

coherent activation of SB channels. In Sec. IV, we propose circuit models for the simulations. Finally, we summarize our results and provide our outlook in Sec. V.

## II. PRELIMINARY NOTIONS

In this section, we briefly recall the quantum steering [2–4] and its associated breaking channels [46,49]. We then introduce the concept of a coherently controlled ancillary system in the sense that a dynamical process of a system is coherently controlled by an ancilla system.

### A. Quantum steering and its associated breaking channel

Given a bipartite state $\rho_{AB}$, satisfying $\rho_{AB} \geqslant 0$ and $\mathrm{Tr}(\rho_{AB}) = 1$, one party (say Alice) aims to steer another party (say Bob) via a set of measurements $\vec{M} := \{M(a|x)\}$ acting on her sharing system; the resulting state is described by

$$\sigma(a|x) = \mathrm{Tr}_A[M(a|x) \otimes \mathbb{1}\rho_{AB}]. \tag{1}$$

The above formula contains both information about the probabilities associated with Alice's measurement results $p(a|x) = \mathrm{Tr}[\sigma(a|x)]$ and Bob's conditional quantum state

$$\rho(a, x) = \sigma(a|x)/\mathrm{Tr}[\sigma(a|x)]. \tag{2}$$

The collections of the (subnormalized) states $\vec{\sigma} = \{\sigma(a|x)\}_{a,x}$ and the measurements $\vec{M} = \{M(a|x)\}_{a,x}$ are called as the *assemblage* and *measurement assemblage*, respectively. A classical description of an assemblage can be described by a local-hidden-state (LHS) model:

$$\sigma(a|x) = \sum_\lambda p(\lambda)p(a|x, \lambda)\sigma_\lambda, \tag{3}$$

where $\sigma_\lambda$ is a predetermined quantum state and $p(a|x, \lambda)$ is a postprocessing with hidden variables $\lambda$. If an assemblage admits an LHS model, it is unsteerable; otherwise, it is steerable. One can use the steering robustness [28] to quantify the quantum steerability:

$$R_S(\vec{\sigma}) = \min\left\{t \middle| \frac{\sigma(a|x) + t\tau(a|x)}{1+t} \text{ admits an LHS model}\right\}, \tag{4}$$

where $t \geqslant 0$ and $\vec{\tau}$ is a noisy assemblage. To generate a steerable assemblage, the measurement assemblage $\vec{M}$ must be incompatible, namely [6–8]

$$M(a|x) \neq \sum_\lambda p(\lambda)p(a|x, \lambda)M_\lambda. \tag{5}$$

Similar to the LHS model, a compatible measurement implies that the measurement assemblage can be described by predetermined measurements $M_\lambda$ with postprocessing and hidden variables.

A quantum channel is described by a completely-positive and trace-preserving map $\Lambda$. We say that $\Lambda$ is SB if the output state $\rho'_{AB} = \Lambda \otimes \mathbb{1}(\rho_{AB})$ always generates unsteerable assemblages for all measurement assemblages $\vec{M}$ and bipartite states $\rho_{AB}$. We denote a channel as $\mathcal{X}$-SB when the channel is SB with a fixed number of inputs $\mathcal{X}$. For instance, if $x \in \{1, 2, 3\}$, such a channel is 3-SB. According to Refs. [46,47], an SB channel is equivalent to an incompatibility-breaking channel in the sense that output measurement assemblages are always compatible for all input measurement assemblages. In other words, it is sufficient to use the maximally entangled state $|\Phi\rangle = \sum_i 1/\sqrt{d}\,|i\rangle\,|i\rangle$ as an input of the channel to test whether the channel is SB or not. This property can be observed via the relation $[M(a|x) \otimes \mathbb{1}](\Lambda \otimes \mathbb{1})\,|\Phi\rangle\langle\Phi| = \Lambda^\dagger[M(a|x)] \otimes \mathbb{1}\,|\Phi\rangle\langle\Phi|$. Here, $d$ is the dimension of the subsystem. Therefore, if the dual map $\Lambda^\dagger$ of a quantum channel $\Lambda$ acting on any measurement assemblage $\vec{M}$ always generates a compatible measurement assemblage, the channel $\Lambda$ is SB or incompatibility breaking.

### B. Coherently controlled ancillary system

Here, we review the concept of the coherently controlled ancillary system of multiple quantum channels. The properties of the coherently controlled ancillary system can be fully characterized when the unitary implementations of the member channels are specified [83]. Consider a set of $N$ quantum channels $\{\Lambda_n\}_{n=1\cdots N}$ that can act on the target system with an initial state $\rho$. According to the Stinespring dilation theorem [84], the channel $\Lambda_n$ can be implemented by introducing an additional environment $\mathcal{E}_n$ prepared in $|E_n\rangle$ and a system-environment global unitary $U_n$, such that

$$U_n(|\psi\rangle \otimes |E_n\rangle) = \sum_i (K_{n,i}\,|\psi\rangle) \otimes |e_{n,i}\rangle \;\forall |\psi\rangle, \tag{6}$$

where $\{|e_{n,i}\rangle\}_i$ is a set of orthonormal states for $\mathcal{E}_n$ and $\{K_{n,i}\}_i$ constitutes a Kraus representation for the channel $\Lambda_n$, i.e., $\Lambda_n(\rho) = \sum_i K_{n,i}\,\rho\,K_{n,i}^\dagger$.

The coherent control of these $N$ channels is achieved by introducing an $N$-dimensional control system C in a state $\rho_C$ and a global unitary $\mathcal{U} = \sum_n |n\rangle\langle n| \otimes U_n$. The output reduced

state of the control-target system can be written as

$$\rho_{\mathrm{CT}} = \mathrm{Tr}_{\{\mathcal{E}_n\}}\left[\mathcal{U}\left(\rho_{\mathrm{C}} \otimes \rho \bigotimes_{l=1}^{N} |E^l\rangle\langle E^l|\right)\mathcal{U}^\dagger\right]. \tag{7}$$

If $\rho_{\mathrm{C}} = |n\rangle\langle n|$, we have $\rho_{\mathrm{CT}} = |n\rangle\langle n| \otimes \Lambda_n(\rho)$. Thus, C can be seen as a classical control determining the specified channel that can be applied to the target system. Further, one can expect that if C is prepared in $\sum_i |i\rangle/\sqrt{N}$, the target system can "pass through" these $N$ quantum channels in a coherent manner. More formally, the output reduced state of the control-target system can be expressed as

$$\rho_{\mathrm{CT}} = \frac{1}{N}\sum_{n=1}^{N} |n\rangle\langle n| \otimes \Lambda_n(\rho) + \sum_{m\neq n} |m\rangle\langle n| \otimes T_m \rho T_n^\dagger. \tag{8}$$

Here, $T_n = \sum_i K_{n,i}\langle E_n|e_{n,i}\rangle$ is called the transformation matrix of the implementation of $\{\Lambda_n\}_n$ [83]. Because we are interested in the target system, before discarding C, one can perform a measurement on C with postselection. Here, it is sufficient to consider the projective measurement $|+\rangle\langle+| = \sum_{i,j}|i\rangle\langle j|/N$ for demonstrating our main results. We also note that this choice of measurement is also applied on different applications of the coherently controlled ancillary system (see Refs. [69,83,85]). The consequent postmeasurement state of the target system then reads

$$\rho_{\mathrm{T}} = \frac{\frac{1}{N}\sum_{n=1}^{N}\Lambda_n(\rho) + \frac{1}{N^2}\sum_{m\neq n} T_m\rho T_n^\dagger}{1 + \frac{1}{N^2}\sum_{m\neq n}\mathrm{Tr}[T_m\rho T_n^\dagger]}. \tag{9}$$

The numerator consists of two terms: The first term characterizes the average effect of these $N$ channels and the second term is characterized by the transformation matrices.

## III. COHERENT ACTIVATION OF STEERABILITY-BREAKING CHANNEL

As mentioned in the introduction, an SB channel can be coherently activated if the SB channel becomes non-SB via the coherently controlled ancillary system. Therefore, an undesired channel *after coherent activation* can now be used to transmit a steerable assemblage. In this section, we provide several concrete examples. In Sec. III A, we analytically show that the SB depolarizing channel can be coherently activated. In addition, when we coherently control multiple copies of the depolarizing channel, one can reliably transmit the steerable resource. In Sec. III B, the numerical calculations indicate that the SB amplitude-damping channel can also be coherently activated.

### A. Depolarizing channel

As a concrete demonstration, we consider the coherent activation of the SB depolarizing channel by the coherently controlled ancillary system. First, we briefly discuss the case without the coherent control. A specific Stinespring dilation of the depolarizing channel $\Lambda^{\mathrm{Dep}}$ can be described by

$$U^{\mathrm{Dep}}|\psi\rangle\otimes|0\rangle = \sqrt{1-\frac{3p}{4}}\,|\psi\rangle\otimes|0\rangle + \sqrt{\frac{p}{4}}\sum_{i=1}^{3}\sigma_i|\psi\rangle\otimes|i\rangle, \tag{10}$$

where $p$ is the visibility of the depolarizing channel, and $\sigma_i$ are Pauli matrices for $i = 1, 2, 3$. Here, $|0\rangle$ and $|i\rangle$ are the input and output states of the extended environment, respectively. In this Stinespring dilation, the Kraus operators of the depolarizing channel can be formulated as

$$K_0^{\mathrm{Dep}} = \sqrt{1-\frac{3p}{4}}\mathbb{1}, \quad K_i^{\mathrm{Dep}} = \sqrt{\frac{p}{4}}\sigma_i, \quad \forall i = 1, 2, 3. \tag{11}$$

In summary, after the above operations, the state is linearly mixed with the maximally mixed state, namely

$$\Lambda^{\mathrm{Dep}}(\rho) = (1-p)\rho + p\mathbb{1}/2. \tag{12}$$

Intuitively, when $p = 1$, any state after the channel becomes the maximally mixed state. Therefore, no information task will have an advantage if one sends the state through this channel. However, if $p = 0$, the channel is the identity channel, which reliably preserves the quantum information. Without loss of generality, for any qubit channel, the visibility can be accessed by performing channel twirling. We describe the physical implementation of the depolarizing channel using a concrete circuit model in Sec. IV.

It has been shown that the depolarizing channel is 2-SB, when $p \geqslant 1 - 1/\sqrt{2}$ [49]. In other words, any assemblage with two measurements cannot be transmitted via the depolarizing channel with the visibility in this range. This threshold can be obtained by considering the maximally entangled state $|\Phi\rangle\langle\Phi|$ with $|\Phi\rangle = \sum_i 1/\sqrt{d}\,|i\rangle|i\rangle$ and measurement assemblage $M(a|x) = \frac{1}{2}(\mathbb{1} + (-1)^a\sigma_x)$ with $a \in \{1, 2\}$ and $x \in \{1, 2\}$. The resulting assemblage is

$$\sigma^{\mathrm{Dep}}(a|x) = (1-p)M(a|x)^T/2 + p\mathbb{1}/4, \tag{13}$$

which is unsteerable when $p \geqslant 1 - 1/\sqrt{2}$. However, the exact boundary between the SB and non-SB depolarizing channel is still an open question [49]. Without loss of generality, we only discuss the two-measurement scenario below. It can be easily extended to the three-measurement scenario.

If the initial state of the control system $\rho_{\mathrm{C}} = \frac{1}{N}\sum_{ij}|i\rangle\langle j|$, by inserting the unitary of the extended environment into Eq. (7), we have

$$\rho_{\mathrm{CT}}^{\mathrm{Dep}} = \frac{1}{N}\mathbb{1}\otimes\Lambda^{\mathrm{Dep}}(\rho) + \frac{1}{N}\sum_{i,j}|i\rangle\langle j|\otimes\left(1-\frac{3p}{4}\right)\Lambda^{\mathrm{Id}}(\rho), \tag{14}$$

where $\Lambda^{\mathrm{Id}}$ denotes the identity channel. After the projective measurement $\sum_{ij}|i\rangle\langle j|/N$ on the control system, the target state becomes

$$\rho_{\mathrm{T}}^{\mathrm{Dep}} = \frac{4\Lambda^{\mathrm{Dep}}(\rho) + (4-3p)(N-1)\Lambda^{\mathrm{Id}}(\rho)}{4 + (4-3p)(N-1)}. \tag{15}$$

The above formula can be seen as a different combination of the depolarizing channel and the identity channel [cf. Eq. (12)].

Next, we discuss the properties of the coherently controlled depolarizing channel described by Eq. (15). Consider that the input state of the target system is the maximally entangled state $\rho = |\Phi\rangle\langle\Phi|$ in Eq. (15). After the channel, Alice performs the Pauli measurements $M(a|x) = \frac{1}{2}(\mathbb{1} + (-1)^a\sigma_x)$ with $a \in \{1, 2\}$ and $x \in \{1, 2\}$. The output state assemblage can be written as

$$\begin{aligned}
&\sigma_{\mathrm{T}}^{\mathrm{Dep}}(a|x) \\
&= \mathrm{Tr}_A\left[M(a|x) \otimes \mathbb{1}\,|\Phi\rangle\langle\Phi|_{\mathrm{T}}^{\mathrm{Dep}}\right] \\
&= \frac{1}{4 + (4-3p)(N-1)}\Big[4\mathrm{Tr}_A\big(M(a|x) \otimes \mathbb{1}\Lambda_A^{\mathrm{Dep}}(|\Phi\rangle\langle\Phi|)\big) \\
&\quad + (4-3p)(N-1)\mathrm{Tr}_A(M(a|x) \otimes \mathbb{1}\,|\Phi\rangle\langle\Phi|)\Big] \\
&= \frac{1}{4 + (4-3p)(N-1)}[4\sigma^{\mathrm{Dep}}(a|x) \\
&\quad + (4-3p)(N-1)\sigma^{\mathrm{Id}}(a|x)], \qquad (16)
\end{aligned}$$

where $\Lambda_A^{\mathrm{Dep}}$ is a shorthand notation for $\Lambda^{\mathrm{Dep}} \otimes \mathbb{1}$, $\sigma^{\mathrm{Dep}}(a|x)$ and $\sigma^{\mathrm{Id}}(a|x)$ denote the assemblage generated by the maximally entangled states after the channels $\Lambda^{\mathrm{Dep}}$ and $\Lambda^{\mathrm{Id}}$, respectively.

We briefly discuss the case with $N$=2 such that

$$\begin{aligned}
\sigma_{\mathrm{T}}^{\mathrm{Dep}}(a|x) &= \frac{1}{8-3p}[4\sigma^{\mathrm{Dep}}(a|x) + (4-3p)\sigma^{\mathrm{Id}}(a|x)], \\
&= \frac{1}{8-3p}\big[(8-7p)M^T(a|x)/2 + p\mathbb{1}\big]. \qquad (17)
\end{aligned}$$

As can be seen, given visibility $p$, the final description in Eq. (17) can be seen as a mixture of $M(a|x)^T$ and $\mathbb{1}/4$ with the "effective" parameter $p' = 4p/(8-3p)$ such that $\sigma^{\mathrm{Dep}}(a|x) = (1-p')M(a|x)^T/2 + p'\mathbb{1}/4$. In this construction, the coherently controlled depolarizing channel is in the same form of the standard depolarizing channel, whereas the visibility $p$ changes to the effective parameter $p'$ by the transformation in Eq. (17). When the visibility $p = 1 - 1/\sqrt{2}$ (the threshold of the 2-SB depolarizing channel), the effective parameter $p' = 0.164$. Because $p' = 0.164 < 1 - 1/\sqrt{2}$, the coherently controlled depolarizing channel is not 2-SB such that the channel can now be used to transmit steerable assemblage. In other words, the SB depolarizing channel is coherently activated. Moreover, one can observe that the threshold of the 2-SB coherently controlled depolarizing channel shifts to $p = 0.48$ with $N = 2$. Recall that when $p \geqslant 1 - 1/\sqrt{2}$ the standard depolarizing channel is SB; otherwise, it is non-2-SB.

Finally, we can see that when the number of copies $N$ the weight on the identity channel [cf. Eqs. (15), and (17)] increases simultaneously. Thus, one can preserve quantum steerability and lead the threshold of the 2-SB coherently controlled depolarizing channel shifts to $p = 0.71$ with $N = 4$. The comparison of the steerability over the $N$ coherently controlled channel is presented in Fig. 2. Moreover, if $N \to \infty$, the coherently controlled channel asymptotically becomes the identity channel.

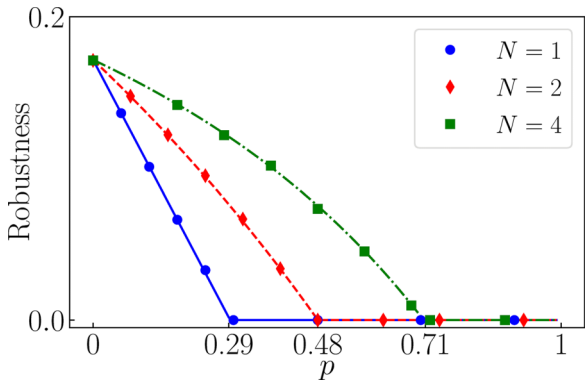


FIG. 2. Steerability over the coherently controlled $N$ depolarizing channel. The simulation results are marked by symbols. When $N = 1$, the system suffers the standard depolarizing channel. The channel is undesired for two measurements (2-SB) after $p \geqslant 1 - 1/\sqrt{2}$. If we apply the concept of coherent control, the quantum-classical boundaries shift to $p = 0.48$ and 0.71 for $N = 2$ and $N = 4$, respectively. Thus, the SB depolarizing channel after the coherent control can now be used to transmit steerable assemblage.

### B. Amplitude-damping channel

Another concrete example is the amplitude-damping channel. The unitaries of the amplitude-damping channel transmit the system $|1\rangle$ to $|0\rangle$ with visibility $\sqrt{1-p}$, while preserving the system $|0\rangle$ with certainty, namely

$$\begin{aligned}
&U^{\mathrm{Amp}}|0\rangle \otimes |0\rangle = |0\rangle \otimes |0\rangle\,, \\
&U^{\mathrm{Amp}}|1\rangle \otimes |0\rangle = \sqrt{1-p}\,|1\rangle \otimes |0\rangle + \sqrt{p}\,|0\rangle \otimes |1\rangle\,. \qquad (18)
\end{aligned}$$

Therefore, the Kraus operators of the amplitude-damping channel can be written as

$$K_0^{\mathrm{Amp}} = \begin{pmatrix} 1 & 0 \\ 0 & \sqrt{1-p} \end{pmatrix}, \quad K_1^{\mathrm{Amp}} = \begin{pmatrix} 0 & \sqrt{p} \\ 0 & 0 \end{pmatrix}. \qquad (19)$$

In summary, the output of the amplitude-damping channel can be expressed as (see also Sec. IV for the physical implementation of the amplitude-damping channel)

$$\Lambda^{\mathrm{Amp}}(\rho) = (1-p)\rho + p\,|0\rangle\langle 0|\,. \qquad (20)$$

The amplitude-damping channel is 2-SB when $p \geqslant 0.5$ because (1) under the two-measurement scenario, the maximal violations of quantum steeraiblity and Bell nonlocality of a quantum state are equivalent [33] and (2) the amplitude-damping channel is Bell nonlocality breaking under the two-measurement scenario if $p \geqslant 0.5$ [49,60,61]. This threshold can be observed when considering, the maximally entangled state and Pauli measurements $\sigma_x$ with $x \in \{1, 2\}$. For more general scenarios, the exact boundary is still unknown. However, it does not change the main statement in this work.

Inserting all the unitaries, the control system, and the extended environment into Eq. (9), the output of the target system can be expressed as

$$\rho_{\mathrm{T}}^{\mathrm{Amp}} = \frac{\Lambda^{\mathrm{Amp}}(\rho) + (N-1)K_0^{\mathrm{Amp}}\rho K_0^{\mathrm{Amp}}}{1 + (N-1)\mathrm{Tr}\big[K_0^{\mathrm{Amp}}\rho K_0^{\mathrm{Amp}}\big]}. \qquad (21)$$

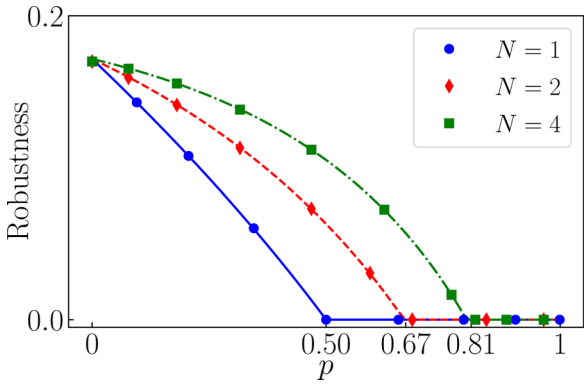


FIG. 3. Steerability over the coherently controlled $N$ amplitude-damping channel. The simulation results are marked by symbols. If $N = 1$, the system suffers from the standard amplitude-damping channel which is undesired (SB) when $p \geqslant 0.5$. The coherently controlled amplitude-damping channels are SB when $p \geqslant 0.67$ and $p \geqslant 0.81$ for $N = 2$ and $N = 4$, respectively. Obviously, with the coherently controlled system, the SB amplitude-damping channel can be activated.

Because the Kraus operator $K_0^{\text{Amp}}$ is full rank, the off-diagonal terms in the state $\rho_{\text{T}}^{\text{AMP}}$ never vanish unless $p = 0$ with the given state $\rho$ with coherency. Compared with the second term in Eq. (20), the Kraus operator $K_0^{\text{Amp}}$ can preserve the coherence of the system.

Now, we consider the input state and the measurement assemblage to be the maximally entangled state and Pauli measurements $\sigma_x$ with $x \in \{1, 2\}$, respectively. We numerically present the steerability over visibility with different numbers of copies $N$ in Fig. 3. One can see that when $N = 2$ and $N = 4$, the SB amplitude-damping channel is coherently activated because the quantum-classical boundaries shift to $p = 0.67$ and $p = 0.81$, respectively. Finally, when $N$ increases, the steering preservability of the coherently controlled amplitude-damping channel is enhanced.

## IV. CIRCUIT SIMULATION

In this section, we present both the controlled depolarizing channel and the controlled amplitude-damping channel with circuit models. Here, we only consider that $N$ is even because we are using multiple qubits as the control system. As the circuit models may be applicable over a wide range of experimental systems, i.e., superconducting and photonic systems, our results are feasible in near-term quantum devices.

Before introducing the circuit models for implementing the controlled channels, we introduce the circuits that are used to demonstrate the Pauli measurements and prepare the maximally entangled state as an input of the target system. We first assume that the initial state of each qubit is in $|0\rangle$, and the measurement gate is always on the computational basis. These two initializations are commonly used in many universal quantum computers, including IBM quantum experience, QuTech, and ionQ [86–90]. The Pauli measurements can be achieved by inserting suitable unitaries before the measurement gate; for instance, measurements on $\sigma_1$ and $\sigma_2$ bases can be demonstrated by rotating the computational basis via $H$ and $S^\dagger H$ gates respectively. Note that $H$ is the Hadamard gate and $S$ is the phase gate, namely

$$H = \frac{1}{\sqrt{2}}\begin{pmatrix} 1 & 1 \\ 1 & -1 \end{pmatrix}, \quad S = \begin{pmatrix} 1 & 0 \\ 0 & i \end{pmatrix}. \tag{22}$$

The maximally entangled state can be generated by operating the Hadamard gate followed by the controlled-NOT (CNOT) gate on state $|00\rangle$. With the maximally entangled state, the Choi state can be obtained by sending Alice's subsystem into the quantum channel. Using the concrete examples mentioned in Sec. III, we describe the detailed implementations of the depolarizing and the amplitude-damping channels in the following subsections.

### A. Circuit model for coherently controlled channels

Here, we introduce a general method to establish the coherently controlled channel (see also the case of $N = 2$ and $\mathcal{X} = 2$ in Fig. 4). If we want to create an $N$ coherently controlled channel, we have to prepare an $N$-dimensional control system in state $\rho_{\text{C}} = \frac{1}{N}\sum_{ij=1}^{N} |i\rangle\langle j|$ and a controlled unitary $\mathcal{U}$. Here, we use $\gamma$ qubits to be the $N$-dimensional control system with $N = 2^\gamma$. However, the number from 1 to $2^\gamma$ in decimal form is represented in binary form with $\gamma$ digits. We show a general circuit model with $\gamma = 2$ ($N = 4$) as an example: $\gamma > 2$ cases can be naturally extended from this. For the $\gamma = 2$ case, we prepare two control qubits in $\frac{1}{4}\sum_{ij=1}^{4} |i\rangle\langle j|$, which can be created by performing Hadamard gates on each qubit. The $\mathcal{U}$ in this case can be written as

$$\begin{aligned} \mathcal{U} = &|0\rangle\langle 0| \otimes |0\rangle\langle 0| \otimes U_{00} \\ &+ |0\rangle\langle 0| \otimes |1\rangle\langle 1| \otimes U_{01} \\ &+ |1\rangle\langle 1| \otimes |0\rangle\langle 0| \otimes U_{10} \\ &+ |1\rangle\langle 1| \otimes |1\rangle\langle 1| \otimes U_{11}. \end{aligned} \tag{23}$$

We note that Eq. (23) can be seen as the operation. It can be decomposed into a series of two-qubits and single-qubit gates [91].

### B. Circuit model for the coherently controlled amplitude-damping channel

Because we introduced the general case of the coherently controlled channel, here, we focus on simulating the amplitude-damping channel with a quantum circuit. The coherently controlled amplitude-damping channel can be obtained by replacing the unitary $U$ in Fig. 4(a) with the unitary $U^{\text{Amp}}$ [see also Fig. 4(b)]. Here, we consider that the input of the target state is $|\psi\rangle$, and the initial state of the environmental system is in $|0\rangle$. We apply a controlled rotation $y$, namely $CR_y(\theta) = |0\rangle\langle 0| \otimes \mathbb{1} + |1\rangle\langle 1| \otimes R_y(\theta)$, followed subsequently with a CNOT operation. Here, $R_y(\theta)$ is a single qubit rotation in the $y$ axis and its matrix form can be written as

$$R_y(\theta) = \begin{pmatrix} \cos\left(\frac{\theta}{2}\right) & -\sin\left(\frac{\theta}{2}\right) \\ \sin\left(\frac{\theta}{2}\right) & \cos\left(\frac{\theta}{2}\right) \end{pmatrix}. \tag{24}$$

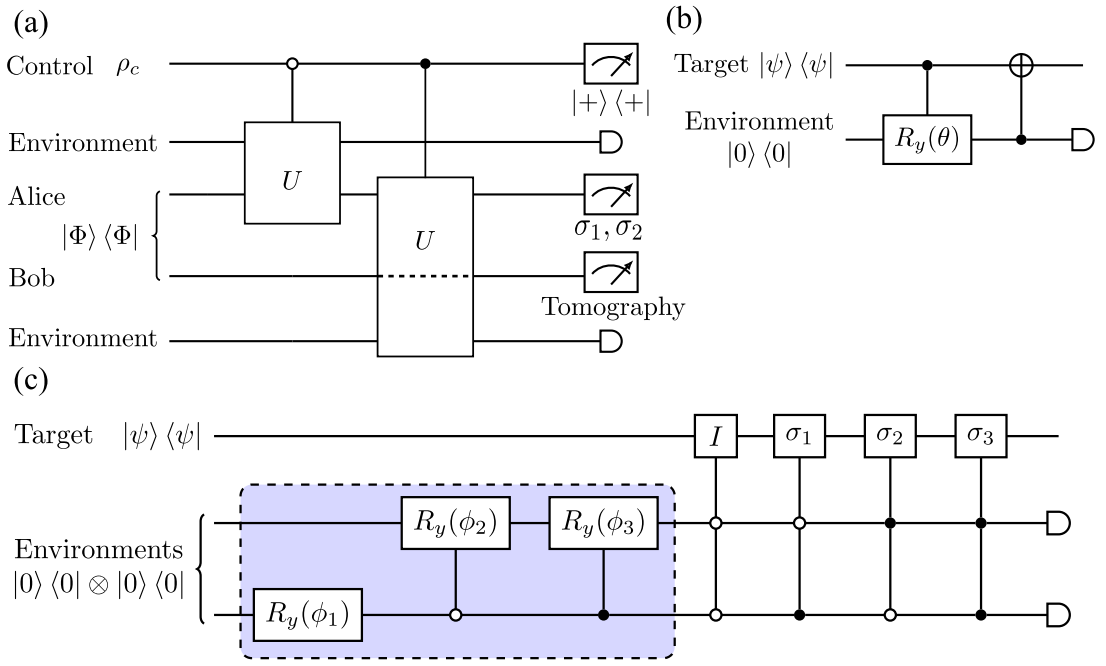


FIG. 4. (a) Circuit model of a coherently controlled channel with $N = 2$ and $\mathcal{X} = 2$. The main idea is using the control system to determine whether the unitary $U$ is acting on the target system. Here, we see that if the control system is in $|0\rangle$ ($|1\rangle$), then the target will be coupled to the first (second) environment. One can use the control system in $|+\rangle$ and measure the control system on the $|+\rangle$ to establish a superposed channel. Note that the white dot in the control system denotes that the unitary is applied when the control system is in $|1\rangle$, and it can be obtained by adding a Pauli-$X$ gate before and after the black dot. (b) Circuit model of an amplitude-damping channel, which can be constructed by a controlled rotation and a CNOT gate. Here, the ancilla qubit is initial in $|0\rangle$. The visibility of amplitude-damping in Eq. (18) can be reformulated by $\theta = 2\arcsin\sqrt{p}$. (c) Circuit model of a depolarizing channel. The two ancillas, being an environment, are initially prepared in $|0\rangle$. By using the (control) rotation $y$ with angles $\phi_1 = 2\arcsin\sqrt{p/2}$, $\phi_2 = 2\arcsin\sqrt{p/(4-2p)}$, and $\phi_3 = \pi/2$, in order, we can construct a state $\sqrt{1-3p/4}\,|0\rangle\,|0\rangle + \sqrt{p/4}(|0\rangle\,|1\rangle + |1\rangle\,|0\rangle + |1\rangle\,|1\rangle)$ (see the colored box). Using this state as a control system and applying controlled-controlled $I$, Pauli-$X$, Pauli-$Y$, and Pauli-$Z$ gates on the target system, the depolarizing channel can be established.

When we apply these gates on the target state, one can easily see that if $\theta = 2\arcsin\sqrt{p}$, this circuit is equivalent to the amplitude-damping channel in Eq. (20). Moreover, the visibility $p$ in the amplitude-damping channel is adjustable by a control-rotation $y$ gate for our circuit implementation. With this circuit, the simulation results of steering robustness under the coherently controlled amplitude-damping channel with $\gamma = 0,\ 1$, and 2 ($N = 1,\ 2$, and 4) are presented in Fig. 3.

### C. Circuit model for the coherently controlled depolarizing channel

We present the coherently controlled depolarizing channel by replacing $U$ in Fig. 4(a) with $U^{\mathrm{Dep}}$. To implement $U^{\mathrm{Dep}}$, we consider a two-qubit system as the environment and apply $R_y(\phi_1)$ followed subsequently by $CR_y(\phi_2)$ and $CR_y(\phi_3)$ in order [see also the colored box in Fig. 4(c)]. After the operations, the environmental state becomes

$$\begin{aligned}|0\rangle\,|0\rangle \to{}& \cos\frac{\phi_1}{2}\cos\frac{\phi_2}{2}\,|0\rangle\,|0\rangle - \cos\frac{\phi_3}{2}\sin\frac{\phi_1}{2}\,|0\rangle\,|1\rangle\\ &- \cos\frac{\phi_1}{2}\sin\frac{\phi_2}{2}\,|1\rangle\,|0\rangle\\ &+ \sin\frac{\phi_3}{2}\sin\frac{\phi_1}{2}\,|1\rangle\,|1\rangle\,. \end{aligned} \tag{25}$$

The visibility $p$ in Eq. (10) is encoded into these three parameters with the relations

$$\begin{aligned}\phi_1 &= 2\arcsin\sqrt{\frac{p}{2}},\\ \phi_2 &= 2\arcsin\sqrt{\frac{p}{(4-2p)}},\\ \phi_3 &= \frac{\pi}{2}.\end{aligned} \tag{26}$$

In other words, the visibility $p$ in the depolarizing channel can be completely determined by the adjustable gates $R_y(\phi_1)$, $CR_y(\phi_2)$, and $CR_y(\phi_3)$ in our circuit construction.

Finally, we use the environmental system as a control system to manipulate the target system. More specifically, we apply controlled-controlled identity, Pauli-$X$, Pauli-$Y$, and Pauli-$Z$ gates on the environmental and target systems. The controlled-controlled operations change the target state to

$$\begin{aligned}|\psi\rangle\otimes|0\rangle\,|0\rangle \to{}& \sqrt{1-\frac{3p}{4}}\,|\psi\rangle\otimes|0\rangle\,|0\rangle + \sqrt{\frac{p}{4}}\sigma_1\,|\psi\rangle\otimes|0\rangle\,|1\rangle\\ &+ \sqrt{\frac{p}{4}}\sigma_2\,|\psi\rangle\otimes|1\rangle\,|0\rangle + \sqrt{\frac{p}{4}}\sigma_3\,|\psi\rangle\otimes|1\rangle\,|1\rangle\,,\end{aligned} \tag{27}$$

which has the same form as Eq. (10), and we can thus simulate the depolarizing channel. The simulation results of steering robustness under the coherently controlled depolarizing channel with $\gamma = 0,\ 1$, and 2 ($N = 1,\ 2$, and 4) are presented in Fig. 2.

## V. DISCUSSION

In this work, we investigated how a coherent control of quantum channels can be used to activate a SB channel. More specifically, we considered two explicit cases, including depolarizing and amplitude-damping channels, because their SB ranges are clearly derived in Refs. [46,49]. We showed that the SB properties of both channels can be coherently activated with two copies of the channels. In this construction, the steerability can be preserved even through the original channel that breaks quantum steerability for any states and measurements. Therefore, the coherently controlled channel can now be applied to steering-based quantum information tasks, i.e., random number generation. If the number of copies increases, the steering preservabilities can be enhanced for both cases. In addition, we constructed the circuit models for both cases and present the simulation results.

This work also highlights the need to consider some research questions. It has been shown that local filtering operations can be used to activate hidden teleportation power [92], hidden steerability [38], and hidden nonlocality [93,94]. Can local filtering operations activate SB channels? Moreover, instead of measuring on the control system, a collective measurement by "untrusted party" on many copies of the unsteerable assemblage can violate the steering inequality [36]. Can a collective measurement activate the SB channels? From the viewpoint of open quantum systems, superposing quantum evolutions can trigger quantum non-Markovain [80,95] and Zeno-like effects [95]. Therefore, it would be worthwhile to explore the impact of these effects on the activation of quantum steerability.

## ACKNOWLEDGMENTS

H.-Y.K. acknowledges partial support from the National Center for Theoretical Sciences and National Science and Technology Council, Taiwan, Grants No. MOST 110-2811-M-006-546 and No. 111-2917-I-564-005. This work is supported partially by the National Center for Theoretical Sciences and National Science and Technology Council, Taiwan, Grant No. MOST 111-2123-M-006-001. H.-Y.K. is partially supported by the Austrian Science Fund (FWF) through Project No. ZK 3 (Zukunftskolleg).

[1] E. Schrödinger, Discussion of probability relations between separated systems, Math. Proc. Camb. Phil. Soc. **31**, 555 (1935).
[2] H. M. Wiseman, S. J. Jones, and A. C. Doherty, Steering, Entanglement, Nonlocality, and the Einstein-Podolsky-Rosen Paradox, Phys. Rev. Lett. **98**, 140402 (2007).
[3] D. Cavalcanti and P. Skrzypczyk, Quantum steering: A review with focus on semidefinite programming, Rep. Prog. Phys. **80**, 024001 (2017).
[4] R. Uola, A. C. S. Costa, H. C. Nguyen, and O. Gühne, Quantum steering, Rev. Mod. Phys. **92**, 015001 (2020).
[5] Y. Xiang, S. Cheng, Q. Gong, Z. Ficek, and Q. He, Quantum steering: Practical challenges and future directions, PRX Quantum **3**, 030102 (2022).
[6] M. T. Quintino, T. Vértesi, and N. Brunner, Joint Measurability, Einstein-Podolsky-Rosen Steering, and Bell Nonlocality, Phys. Rev. Lett. **113**, 160402 (2014).
[7] R. Uola, T. Moroder, and O. Gühne, Joint Measurability of Generalized Measurements Implies Classicality, Phys. Rev. Lett. **113**, 160403 (2014).
[8] R. Uola, C. Budroni, O. Gühne, and J.-P. Pellonpää, One-to-One Mapping between Steering and Joint Measurability Problems, Phys. Rev. Lett. **115**, 230402 (2015).
[9] O. Gühne, E. Haapasalo, T. Kraft, J.-P. Pellonpää, and R. Uola, Colloquium: Incompatible measurements in quantum information science, Rev. Mod. Phys. **95**, 011003 (2023).
[10] H.-Y. Ku, C.-Y. Hsieh, S.-L. Chen, Y.-N. Chen, and C. Budroni, Complete classification of steerability under local filters and its relation with measurement incompatibility, Nat. Commun. **13**, 4973 (2022).
[11] M. F. Pusey, Negativity and steering: A stronger Peres conjecture, Phys. Rev. A **88**, 032313 (2013).
[12] D. Cavalcanti and P. Skrzypczyk, Quantitative relations between measurement incompatibility, quantum steering, and nonlocality, Phys. Rev. A **93**, 052112 (2016).
[13] M. Fadel and M. Gessner, Entanglement of local hidden states, Quantum **6**, 651 (2022).
[14] N. Brunner, D. Cavalcanti, S. Pironio, V. Scarani, and S. Wehner, Bell nonlocality, Rev. Mod. Phys. **86**, 419 (2014).
[15] S.-L. Chen, C. Budroni, Y.-C. Liang, and Y.-N. Chen, Natural Framework for Device-Independent Quantification of Quantum Steerability, Measurement Incompatibility, and Self-Testing, Phys. Rev. Lett. **116**, 240401 (2016).
[16] M. T. Quintino, C. Budroni, E. Woodhead, A. Cabello, and D. Cavalcanti, Device-Independent Tests of Structures of Measurement Incompatibility, Phys. Rev. Lett. **123**, 180401 (2019).
[17] S.-L. Chen, H.-Y. Ku, W. Zhou, J. Tura, and Y.-N. Chen, Robust self-testing of steerable quantum assemblages and its applications on device-independent quantum certification, Quantum **5**, 552 (2021).
[18] D. J. Saunders, S. J. Jones, H. M. Wiseman, and G. J. Pryde, Experimental EPR-steering using Bell-local states, Nat. Phys. **6**, 845 (2010).
[19] A. J. Bennet, D. A. Evans, D. J. Saunders, C. Branciard, E. G. Cavalcanti, H. M. Wiseman, and G. J. Pryde, Arbitrarily Loss-Tolerant Einstein-Podolsky-Rosen Steering Allowing a Demonstration Over 1 km of Optical Fiber with no Detection Loophole, Phys. Rev. X **2**, 031003 (2012).
[20] S. Wollmann, N. Walk, A. J. Bennet, H. M. Wiseman, and G. J. Pryde, Observation of Genuine One-Way Einstein-Podolsky-Rosen Steering, Phys. Rev. Lett. **116**, 160403 (2016).

[21] Y.-Y. Zhao, H.-Y. Ku, S.-L. Chen, H.-B. Chen, F. Nori, G.-Y. Xiang, C.-F. Li, G.-C. Guo, and Y.-N. Chen, Experimental demonstration of measurement-device-independent measure of quantum steering, npj Quantum Inf. **6**, 77 (2020).

[22] S. Wollmann, R. Uola, and A. C. S. Costa, Experimental Demonstration of Robust Quantum Steering, Phys. Rev. Lett. **125**, 020404 (2020).

[23] X. Deng, Y. Liu, M. Wang, X. Su, and K. Peng, Sudden death and revival of Gaussian Einstein–Podolsky–Rosen steering in noisy channels, npj Quantum Inf. **7**, 65 (2021).

[24] Y.-Y. Zhao, C. Zhang, S. Cheng, X. Li, Y. Guo, B.-H. Liu, H.-Y. Ku, S.-L. Chen, Q. Wen, Y.-F. Huang, G.-Y. Xiang, C.-F. Li, and G.-C. Guo, Device-independent verification of Einstein–Podolsky–Rosen steering, Optica **10**, 66 (2023).

[25] C. Branciard, E. G. Cavalcanti, S. P. Walborn, V. Scarani, and H. M. Wiseman, One-sided device-independent quantum key distribution: Security, feasibility, and the connection with steering, Phys. Rev. A **85**, 010301(R) (2012).

[26] P. Skrzypczyk and D. Cavalcanti, Maximal Randomness Generation from Steering Inequality Violations Using Qudits, Phys. Rev. Lett. **120**, 260401 (2018).

[27] Y. Guo, S. Cheng, X. Hu, B.-H. Liu, E.-M. Huang, Y.-F. Huang, C.-F. Li, G.-C. Guo, and E. G. Cavalcanti, Experimental Measurement-Device-Independent Quantum Steering and Randomness Generation Beyond Qubits, Phys. Rev. Lett. **123**, 170402 (2019).

[28] M. Piani and J. Watrous, Necessary and Sufficient Quantum Information Characterization of Einstein-Podolsky-Rosen Steering, Phys. Rev. Lett. **114**, 060404 (2015).

[29] K. Sun, X.-J. Ye, Y. Xiao, X.-Y. Xu, Y.-C. Wu, J.-S. Xu, J.-L. Chen, C.-F. Li, and G.-C. Guo, Demonstration of Einstein–Podolsky–Rosen steering with enhanced subchannel discrimination, npj Quantum Inf. **4**, 12 (2018).

[30] B. Yadin, M. Fadel, and M. Gessner, Metrological complementarity reveals the Einstein-Podolsky-Rosen paradox, Nat. Commun. **12**, 2410 (2021).

[31] P. Skrzypczyk, M. Navascués, and D. Cavalcanti, Quantifying Einstein-Podolsky-Rosen Steering, Phys. Rev. Lett. **112**, 180404 (2014).

[32] R. Gallego and L. Aolita, Resource Theory of Steering, Phys. Rev. X **5**, 041008 (2015).

[33] A. C. S. Costa and R. M. Angelo, Quantification of Einstein-Podolsky-Rosen steering for two-qubit states, Phys. Rev. A **93**, 020103(R) (2016).

[34] K. Sun, X.-J. Ye, J.-S. Xu, X.-Y. Xu, J.-S. Tang, Y.-C. Wu, J.-L. Chen, C.-F. Li, and G.-C. Guo, Experimental Quantification of Asymmetric Einstein-Podolsky-Rosen Steering, Phys. Rev. Lett. **116**, 160404 (2016).

[35] H.-Y. Ku, S.-L. Chen, C. Budroni, A. Miranowicz, Y.-N. Chen, and F. Nori, Einstein-Podolsky-Rosen steering: Its geometric quantification and witness, Phys. Rev. A **97**, 022338 (2018).

[36] M. T. Quintino, N. Brunner, and M. Huber, Superactivation of quantum steering, Phys. Rev. A **94**, 062123 (2016).

[37] C.-Y. Hsieh, Y.-C. Liang, and R.-K. Lee, Quantum steerability: Characterization, quantification, superactivation, and unbounded amplification, Phys. Rev. A **94**, 062120 (2016).

[38] T. Pramanik, Y.-W. Cho, S.-W. Han, S.-Y. Lee, Y.-S. Kim, and S. Moon, Revealing hidden quantum steerability using local filtering operations, Phys. Rev. A **99**, 030101(R) (2019).

[39] R. V. Nery, M. M. Taddei, P. Sahium, S. P. Walborn, L. Aolita, and G. H. Aguilar, Distillation of Quantum Steering, Phys. Rev. Lett. **124**, 120402 (2020).

[40] S. Gupta, D. Das, and A. S. Majumdar, Distillation of genuine tripartite Einstein-Podolsky-Rosen steering, Phys. Rev. A **104**, 022409 (2021).

[41] Y. Liu, K. Zheng, H. Kang, D. Han, M. Wang, L. Zhang, X. Su, and K. Peng, Distillation of Gaussian Einstein-Podolsky-Rosen steering with noiseless linear amplification, npj Quantum Inf. **8**, 38 (2022).

[42] Y.-N. Chen, C.-M. Li, N. Lambert, S.-L. Chen, Y. Ota, G.-Y. Chen, and F. Nori, Temporal steering inequality, Phys. Rev. A **89**, 032112 (2014).

[43] M. Piani, Channel steering, J. Opt. Soc. Am. B **32**, A1 (2015).

[44] M. F. Pusey, Verifying the quantumness of a channel with an untrusted device, J. Opt. Soc. Am. B **32**, A56 (2015).

[45] H.-Y. Ku, S.-L. Chen, N. Lambert, Y.-N. Chen, and F. Nori, Hierarchy in temporal quantum correlations, Phys. Rev. A **98**, 022104 (2018).

[46] T. Heinosaari, J. Kiukas, D. Reitzner, and J. Schultz, Incompatibility breaking quantum channels, J. Phys. A: Math. Theor. **48**, 435301 (2015).

[47] J. Kiukas, C. Budroni, R. Uola, and J.-P. Pellonpää, Continuous-variable steering and incompatibility via state-channel duality, Phys. Rev. A **96**, 042331 (2017).

[48] L. Guerini, M. T. Quintino, and L. Aolita, Distributed sampling, quantum communication witnesses, and measurement incompatibility, Phys. Rev. A **100**, 042308 (2019).

[49] H.-Y. Ku, J. Kadlec, A. Černoch, M. T. Quintino, W. Zhou, K. Lemr, N. Lambert, A. Miranowicz, S.-L. Chen, F. Nori, and Y.-N. Chen, Quantifying quantumness of channels without entanglement, PRX Quantum **3**, 020338 (2022).

[50] M. B. Ruskai, Qubit entanglement breaking channels, Rev. Math. Phys. **15**, 643 (2003).

[51] M. Horodecki, P. W. Shor, and M. B. Ruskai, Entanglement breaking channels, Rev. Math. Phys. **15**, 629 (2003).

[52] M. Girard, M. Plávala, and J. Sikora, Jordan products of quantum channels and their compatibility, Nat. Commun. **12**, 2129 (2021).

[53] M. Ioannou, P. Sekatski, S. Designolle, B. D. M. Jones, R. Uola, and N. Brunner, Simulability of High-Dimensional Quantum Measurements, Phys. Rev. Lett. **129**, 190401 (2022).

[54] B. D. M. Jones, R. Uola, T. Cope, M. Ioannou, S. Designolle, P. Sekatski, and N. Brunner, Equivalence between simulability of high-dimensional measurements and high-dimensional steering, arXiv:2207.04080 [quant-ph].

[55] R. Uola, F. Lever, O. Gühne, and J.-P. Pellonpää, Unified picture for spatial, temporal, and channel steering, Phys. Rev. A **97**, 032301 (2018).

[56] K. C. V. Jiráková, A. Černoch, K. Lemr, K. Bartkiewicz, and A. Miranowicz, Experimental hierarchy and optimal robustness of quantum correlations of two-qubit states with controllable white noise, Phys. Rev. A **104**, 062436 (2021).

[57] D. Rosset, F. Buscemi, and Y.-C. Liang, Resource Theory of Quantum Memories and their Faithful Verification with Minimal Assumptions, Phys. Rev. X **8**, 021033 (2018).

[58] X. Yuan, Y. Liu, Q. Zhao, B. Regula, J. Thompson, and M. Gu, Universal and operational benchmarking of quantum memories, npj Quantum Inf. **7**, 108 (2021).

[59] P. Lipka-Bartosik, A. F. Ducuara, T. Purves, and P. Skrzypczyk, Operational significance of the quantum resource theory of Buscemi nonlocality, PRX Quantum **2**, 020301 (2021).

[60] R. Pal and S. Ghosh, Non-locality breaking qubit channels: The case for CHSH inequality, J. Phys. A: Math. Theor. **48**, 155302 (2015).

[61] Y. Zhang, R. A. Bravo, V. O. Lorenz, and E. Chitambar, Channel activation of CHSH nonlocality, New J. Phys. **22**, 043003 (2020).

[62] S. Kumari, J. Naikoo, S. Ghosh, and A. K. Pan, Interplay of nonlocality and incompatibility breaking qubit channels, Phys. Rev. A **107**, 022201 (2023).

[63] D. K. L. Oi, Interference of Quantum Channels, Phys. Rev. Lett. **91**, 067902 (2003).

[64] N. Gisin, N. Linden, S. Massar, and S. Popescu, Error filtration and entanglement purification for quantum communication, Phys. Rev. A **72**, 012338 (2005).

[65] M. M. Taddei, J. Cariñe, D. Martínez, T. García, N. Guerrero, A. A. Abbott, M. Araújo, C. Branciard, E. S. Gómez, S. P. Walborn, L. Aolita, and G. Lima, Computational advantage from the quantum superposition of multiple temporal orders of photonic gates, PRX Quantum **2**, 010320 (2021).

[66] J. Wechs, H. Dourdent, A. A. Abbott, and C. Branciard, Quantum circuits with classical versus quantum control of causal order, PRX Quantum **2**, 030335 (2021).

[67] J. Barrett, R. Lorenz, and O. Oreshkov, Cyclic quantum causal models, Nat. Commun. **12**, 885 (2021).

[68] B. Regula and R. Takagi, Fundamental limitations on distillation of quantum channel resources, Nat. Commun. **12**, 4411 (2021).

[69] G. Chiribella and H. Kristjánsson, Quantum Shannon theory with superpositions of trajectories, Proc. R. Soc. A. **475**, 20180903 (2019).

[70] J. Miguel-Ramiro, A. Pirker, and W. Dür, Genuine quantum networks with superposed tasks and addressing, npj Quantum Inf. **7**, 135 (2021).

[71] S. S. Bhattacharya, A. G. Maity, T. Guha, G. Chiribella, and M. Banik, Random-receiver quantum communication, PRX Quantum **2**, 020350 (2021).

[72] M. Nery, M. T. Quintino, P. A. Guérin, T. O. Maciel, and R. O. Vianna, Simple and maximally robust processes with no classical common-cause or direct-cause explanation, Quantum **5**, 538 (2021).

[73] M. T. Quintino and D. Ebler, Deterministic transformations between unitary operations: Exponential advantage with adaptive quantum circuits and the power of indefinite causality, Quantum **6**, 679 (2022).

[74] K.-Y. Lee, J.-D. Lin, A. Miranowicz, F. Nori, H.-Y. Ku, and Y.-N. Chen, Steering-enhanced quantum metrology using superpositions of noisy phase shifts, Phys. Rev. Res. **5**, 013103 (2023).

[75] J. Foo, R. B. Mann, and M. Zych, Entanglement amplification between superposed detectors in flat and curved spacetimes, Phys. Rev. D **103**, 065013 (2021).

[76] J. Foo, S. Onoe, and M. Zych, Unruh-deWitt detectors in quantum superpositions of trajectories, Phys. Rev. D **102**, 085013 (2020).

[77] L. J. Henderson, A. Belenchia, E. Castro-Ruiz, C. Budroni, M. Zych, Č. Brukner, and R. B. Mann, Quantum Temporal Superposition: The Case of Quantum Field Theory, Phys. Rev. Lett. **125**, 131602 (2020).

[78] M. Ban, Relaxation process of a two-level system in a coherent superposition of two environments, Quantum Inf. Process **19**, 351 (2020).

[79] M. Ban, Two-qubit correlation in two independent environments with indefiniteness, Phys. Lett. A **385**, 126936 (2021).

[80] O. Siltanen, T. Kuusela, and J. Piilo, Interferometric approach to open quantum systems and non-Markovian dynamics, Phys. Rev. A **103**, 032223 (2021).

[81] S. Milz, J. Bavaresco, and G. Chiribella, Resource theory of causal connection, Quantum **6**, 788 (2022).

[82] C.-Y. Hsieh, Resource preservability, Quantum **4**, 244 (2020).

[83] A. A. Abbott, J. Wechs, D. Horsman, M. Mhalla, and C. Branciard, Communication through coherent control of quantum channels, Quantum **4**, 333 (2020).

[84] W. F. Stinespring, Positive functions on $C^*$-algebras, Proc. Amer. Math. Soc. **6**, 211 (1955).

[85] N. Loizeau and A. Grinbaum, Channel capacity enhancement with indefinite causal order, Phys. Rev. A **101**, 012340 (2020).

[86] IBM Quantum Services, https://quantum-computing.ibm.com/services?services=systems&system.

[87] H.-Y. Ku, N. Lambert, F.-J. Chan, C. Emary, Y.-N. Chen, and F. Nori, Experimental test of non-macrorealistic cat states in the cloud, npj Quantum Inf. **6**, 98 (2020).

[88] N. M. P. Neumann, Classification using a two-qubit quantum chip, in *Computational Science – ICCS 2021*, edited by M. Paszynski, D. Kranzlmüller, V. V. Krzhizhanovskaya, J. J. Dongarra, and P. M. A. Sloot (Springer International, Cham, 2021), pp. 74–83.

[89] Y. Alexeev, D. Bacon, K. R. Brown, R. Calderbank, L. D. Carr, F. T. Chong, B. DeMarco, D. Englund, E. Farhi, B. Fefferman, A. V. Gorshkov, A. Houck, J. Kim, S. Kimmel, M. Lange, S. Lloyd, M. D. Lukin, D. Maslov, P. Maunz, C. Monroe *et al.*, Quantum computer systems for scientific discovery, PRX Quantum **2**, 017001 (2021).

[90] E. Altman, K. R. Brown, G. Carleo, L. D. Carr, E. Demler, C. Chin, B. DeMarco, S. E. Economou, M. A. Eriksson, Kai-Mei C. Fu, M. Greiner, K. R. A. Hazzard, R. G. Hulet, A. J. Kollár, B. L. Lev, M. D. Lukin, R. Ma, X. Mi, S. Misra, C. Monroe *et al.*, Quantum simulators: Architectures and opportunities, PRX Quantum **2**, 017003 (2021).

[91] M. A. Nielsen and I. L. Chuang, *Quantum Computation and Quantum Information: 10th Anniversary Edition* (Cambridge University Press, Cambridge, UK, 2011).

[92] J.-Y. Li, X.-X. Fang, T. Zhang, Gelo Noel M. Tabia, H. Lu, and Y.-C. Liang, Activating hidden teleportation power: Theory and experiment, Phys. Rev. Res. **3**, 023045 (2021).

[93] N. Gisin, Hidden quantum nonlocality revealed by local filters, Phys. Lett. A **210**, 151 (1996).

[94] F. Hirsch, M. T. Quintino, J. Bowles, and N. Brunner, Genuine Hidden Quantum Nonlocality, Phys. Rev. Lett. **111**, 160402 (2013).

[95] J.-D. Lin, C.-Y. Huang, N. Lambert, G.-Y. Chen, F. Nori, and Y.-N. Chen, Space-time dual quantum zeno effect: Interferometric engineering of open quantum system dynamics, Phys. Rev. Res. **4**, 033143 (2022).